MOLECULAR AND CELLULAR BIOLOGY, Dec. 2001, p. 8117–8128 Vol. 21, No. 23
0270-7306/01/$04.00+0 DOI: 10.1128/MCB.21.23.8117–8128.2001

Telomere Formation by Rap1p Binding Site Arrays Reveals End-Specific Length Regulation Requirements and Active Telomeric Recombination

SIMONA GROSSI, ALESSANDRO BIANCHI, PASCAL DAMAY, AND DAVID SHORE*

Department of Molecular Biology, University of Geneva, 1211 Geneva 4, Switzerland

Received 13 June 2001/Returned for modification 11 July 2001/Accepted 29 August 2001

Rap1p, the major telomere repeat binding protein in yeast, has been implicated in both de novo telomere formation and telomere length regulation. To characterize the role of Rap1p in these processes in more detail, we studied the generation of telomeres in vivo from linear DNA substrates containing defined arrays of Rap1p binding sites. Consistent with previous work, our results indicate that synthetic Rap1p binding sites within the internal half of a telomeric array are recognized as an integral part of the telomere complex in an orientation-independent manner that is largely insensitive to the precise spacing between adjacent sites. By extending the lengths of these constructs, we found that several different Rap1p site arrays could never be found at the very distal end of a telomere, even when correctly oriented. Instead, these synthetic arrays were always followed by a short (≈100-bp) "cap" of genuine TG repeat sequence, indicating a remarkably strict sequence requirement for an end-specific function(s) of the telomere. Despite this fact, even misoriented Rap1p site arrays promote telomere formation when they are placed at the distal end of a telomere-healing substrate, provided that at least a single correctly oriented site is present within the array. Surprisingly, these heterogeneous arrays of Rap1p binding sites generate telomeres through a *RAD52*-dependent fusion resolution reaction that results in an inversion of the original array. Our results provide new insights into the nature of telomere end capping and reveal one way by which recombination can resolve a defect in this process.

Telomeres, the specialized protein-DNA complexes that constitute the ends of eukaryotic chromosomes, permit the complete replication of chromosome ends and allow the cell to distinguish these natural ends from accidental DNA breaks (reviewed recently in reference 27). The complete replication of telomeric DNA, which cannot be accomplished by conventional DNA polymerases, is carried out in most organisms by a cellular reverse transcriptase, called telomerase, that carries its own RNA template (42). Telomerase generates simple repeat sequences (TTAGGG in mammals and most other eukaryotes but $TG_{1–3}$ in the yeast *Saccharomyces cerevisiae*) in which the GT-rich strand forms the 3′ end of the chromosome. $TG_{1–3}$ repeat tracts in yeast, which vary in length from ≈250 to 350 bp, form very high affinity binding sites for the multifunctional regulatory protein Rap1 (26). Because of the irregular nature of the repeats, the disposition of Rap1p binding sites does not appear to be constant, though an average of one site per ≈18 bp has been measured in one study (11). In mammalian cells, the regular TTAGGG telomeric repeats are longer (and more heterogeneous in length) than the related repeats in yeast (≈10 kb in humans and up to 50 kb in the mouse, *Mus musculus*). Telomere repeat DNA in mammalian cells is bound by at least two distinct, related proteins, TRF1 and TRF2 (2, 4, 7).

The unusual mechanism of telomere DNA replication imposes a regulatory problem on the cell. Telomerase addition must be sufficient to counteract either replicative loss or degradation of terminal sequences, yet unregulated addition of repeats can be detrimental to cell growth (36, 49). Consequently, telomere length is regulated about a fixed average value. This fact implies a cellular mechanism to measure telomere length and to then regulate telomerase addition, end degradation, or both, accordingly. Recent studies of both yeast and mammalian cells suggest that this is accomplished, at least in part, by a negative-feedback system involving the telomere repeat binding proteins (34, 46, 50, 54) that is likely to act in *cis* on the telomerase complex (33). These studies suggest that the metric of telomere length is not the TG repeat tract per se but rather the number of proteins bound to it. In yeast, a complex between Rap1p and two interacting factors, Rif1p and Rif2p (15, 58), may generate a number-dependent structural transition that controls telomerase access or activity at the telomere (48). Interestingly, Rap1p also appears to be directly involved in promoting the de novo formation of telomeres at DNA ends in vivo (30, 31, 45).

Here we have examined in more detail the role of Rap1p in telomere formation and length regulation by using arrays of synthetic Rap1p binding sites of varying number, spacing, and orientation to generate telomeres in vivo. This has allowed us to study telomeres composed, at least in part, of a defined arrangement of Rap1p binding sites, a situation that cannot be attained with the native $TG_{1–3}$ repeats of *S. cerevisiae*. Our results extend previous work (34, 45, 46) by demonstrating a certain degree of flexibility in the sequence, spacing, and orientation requirements for Rap1p binding sites when the synthetic arrays contain fewer binding sites than a native telomere. In addition, we found an unexpected sensitivity of either the length regulation or telomerase addition mechanisms to the precise sequence present at the extreme end of a telomeric array. For example, several Rap1p site arrays that contributed

* Corresponding author. Mailing address: Department of Molecular Biology, University of Geneva, 30, Quai Ernest-Ansermet, 1211 Geneva 4, Switzerland. Phone: 41-22-702-6183. Fax: 41-22-702-6868. E-mail: David.Shore@molbio.unige.ch.

to telomere length regulation when present within the internal half of a telomere failed to do so when present distally and were never recovered at the very end of a telomere. Likewise, "misoriented" arrays, in which the CA-rich sequence was present on the 3′ end, contributed to telomere length regulation only when present internally. Strikingly, however, misoriented arrays made a quantitative contribution to telomere healing regardless of their location (proximal or distal) in the healing substrate as long as they were present together with at least one correctly oriented site. Examination of the telomeres resulting from substrates with distal misoriented sites revealed a robust mechanism of sequence rearrangement between telomeric repeats. We discuss these results in terms of models for a special role of the end in telomere length regulation and in the formation of a "cap" structure that protects the chromosome end from DNA recombination and repair machinery.

MATERIALS AND METHODS

Yeast strains and methods. All strains employed were derivatives of W303-1B (*MAT*α *leu2-3*, *112 his3-11*, *15 ura3-1*, *ade2-1*, *trp1-1*, *can1-100*) (53). Standard methods for yeast growth and manipulation were used throughout (1). Strain YS293, used in HO cutting experiments, is derived from a *RAD5* version of W303-1B (a generous gift of Hannah Klein). It carries a partial deletion of the Y alpha and Z1 regions at the *MAT* locus, which eliminates the HO recognition site, and contains a copy of the HO endonuclease gene, driven by the *GAL1* promoter and integrated at the *HIS3* locus. An HO cleavage site was introduced into this strain at the *ADH4* locus by transformation with *Sac*I-*Kpn*I-cleaved pGS45. YS312 is derived from YS293 by replacement of the *RAD52* gene by *KanMX4*. Details of these constructs are available upon request.

Plasmids. Telomere-healing constructs containing Rap1p binding site array constructs were made using a modified version of pADH4UCA (12) in which an oligonucleotide encoding *Bam*HI, *Bgl*II, and *Kpn*I sites was introduced into the unique *Bam*HI site. Oligonucleotides encoding Rap1p binding sites were introduced between the *Bam*HI and *Bgl*II sites, and head-to-tail arrays were generated by a reiterative cloning strategy, details of which are available upon request, in which *Bam*HI and *Bgl*II sites were directly joined. The DNA sequences of the binding site oligonucleotides are as follows (the consensus Rap1p binding site sequences are underlined, and the *Bam*HI overhangs are in parentheses): dimer 15- and 20-bp spacing sites, 5′(GATC)CTACACCCATACACCTTACACCCAGACACCA3′; 17-bp spacing site, 5′(GATC)CACACCCATACAA3′; 22-bp spacing site, 5′(GATC)CGTACACCCATACATCGA3′; 27-bp spacing site, 5′(GATC)CTGTGTACACCCATACATCGTCA3′; 31-bp spacing site, 5′(GATC)CGTGTTGACACCCATACATTGGTGATA3′. The complements of these oligonucleotides begin with the sequence 5′(GATC)3′, which forms the *Bgl*II-compatible end, and lack sequences complementary to the GATC sequence at the 5′ end of the first set. Annealing of the complementary oligonucleotides produces a duplex that will anneal to and restore a *Bam*HI site at one end and a *Bgl*II site at the other end. The sequence between the native TG repeat and the most proximal *Bam*HI restriction site (or *Bgl*II, in the case of misoriented Rap1p site arrays) is 5′ TCTCTCACATCTACCTCTACTCTG(GGATCC) 3′ and is the same for all of the constructs tested.

Plasmid pGS45, used to generate a novel HO cut site near the left arm of chromosome VII, contains the following elements inserted between the *Kpn*I and *Sac*I sites of pBluescript KS(+): a region of homology to the *MNT2* gene, the *URA3* gene, a 24-bp recognition site for the HO endonuclease, an array of 12 misoriented Rap1 binding sites followed by 2 correctly oriented Rap1 binding sites, the *ADE2* gene, and a region of homology to the *ADH4* gene (see Fig. 7). Transformation with the *Sac*I/*Kpn*I-digested plasmid results in the replacement of sequences between *MNT2* and *ADH4* at chromosome VII-L with the *Kpn*I-*Sac*I insert. Both the *MNT2* and *ADH4* open reading frames are disrupted as a consequence. Additional details of this plasmid are available upon request.

Telomere Southern blots and telomere length measurements. Yeast DNA was isolated from overnight cultures, and 1 μg was digested with the appropriate enzymes. DNA fragments were separated by electrophoresis in 1.5% agarose gels, transferred to HyBond N+ membranes, and hybridized to random-primed probes (either a 1.1-kb *URA3* or a 0.5-kb *ADE2* fragment) by standard procedures. The membranes were then autoradiographed on X-ray film or with a phosphorimager (Bio-Rad Molecular Imager FX). The midpoints of the telomere band distributions were determined with the Bio-Rad Quantity One program, using the internal *ura3-1* control band in each lane as a size reference. The values reported are averages of at least two independent transformants. The variation between different clones was typically <10% of the total telomere tract length, and often <5%.

Telomere-healing assays. Yeast transformations to measure telomere-healing efficiency were done using the "best" LiOAc method of Gietz and coworkers (http://www.umanitoba.ca/faculties/medicine/biochem/gietz/Trafo.html). In order to compare the telomere-healing efficiencies of different plasmids, competent cells (aliquots of the same culture) were transformed with equivalent amounts of different plasmids digested with the appropriate enzymes to generate a linear DNA fragment with Rap1p binding sites at one end, *URA3* in the middle, and a fragment of *ADH4* at the other end. The *ADH4* end directs homologous recombination to the endogenous *ADH4* locus on chromosome VII-L, replacing the ≈20 kb of sequence between *ADH4* and the native chromosome VII-L telomere (12). Cells were plated on synthetic complete (SC) medium lacking uracil (SC-Ura), and Ura^+ transformants were replicated on SC plates containing 1 g of 5-fluoroorotic acid (FOA)/liter. The number of Ura^+ and FOA^r colonies was taken as a measure of telomere formation at the *ADH4* locus. The experiment was repeated three times for each plasmid, and the average values were calculated after normalization to the number of Leu^+ colonies arising from transformation of the same batch of competent cells with the plasmid pRS315 (*LEU2 CENVI*).

For HO endonuclease induction, cells were grown in preinduction medium (yeast extract-peptone [YP] plus 2% glucose) at 30°C to a density of 5×10^6/ml, washed, and resuspended in YP plus 2% galactose. Samples were removed at the indicated time points, and genomic DNA was prepared and analyzed by Southern blotting using a 0.5-kb *ADE2* hybridization probe as described above.

RESULTS

Generation of telomeres from synthetic arrays of Rap1p binding sites. To begin to examine more systematically the role of Rap1p in telomere formation and length regulation, we constructed and tested sets of telomere-healing substrates (12) containing tandem arrays of Rap1p binding sites with varied site orientation and spacing. The first series of arrays that we tested was based upon a 35-bp oligonucleotide containing two consensus Rap1p binding sites (5, 13) whose sequence deviates from the strict GT/AC strand bias of native telomere repeats at a single position within each binding site and within both flanking spacer regions. We used a reiterative cloning strategy (see Materials and Methods) to generate head-to-tail arrays with 2, 4, 8, and 16 copies of this oligonucleotide (4, 8, 16, and 32 binding sites) in either a native ("correct") orientation, in which the TG-rich strand runs 5′ to 3′ towards the healing end, or a misoriented configuration (Fig. 1A). In both cases the synthetic arrays were followed by a short 80-bp tract of correctly oriented, native TG_{1-3} repeat "seed" sequence. Because of the precise disposition of the two Rap1p binding sites in the original oligonucleotide, the arrays have an alternating 15- and 20-bp spacing between adjacent sites.

After transformation and selection for Ura^+ clones, the new telomeres generated from these synthetic arrays were examined by Southern blotting with a *URA3* probe (Fig. 1A). Digestion with *Hin*dIII yields two hybridizing fragments: one containing the telomeric *URA3* gene and the other containing the endogenous *ura3* gene, which serves as an internal size marker. A double digestion with either *Hin*dIII and *Bam*HI (for the correctly oriented arrays) or *Hin*dIII and *Bgl*II (for the misoriented arrays) allows us to determine whether the healed telomeres still contain the complete synthetic array of Rap1p binding sites adjacent to *URA3*. The difference between the average *Hin*dIII fragment size and the size of the *Hin*dIII-plus-*Bam*HI (or *Hin*dIII-plus-*Bgl*II) fragments provides an indirect measure

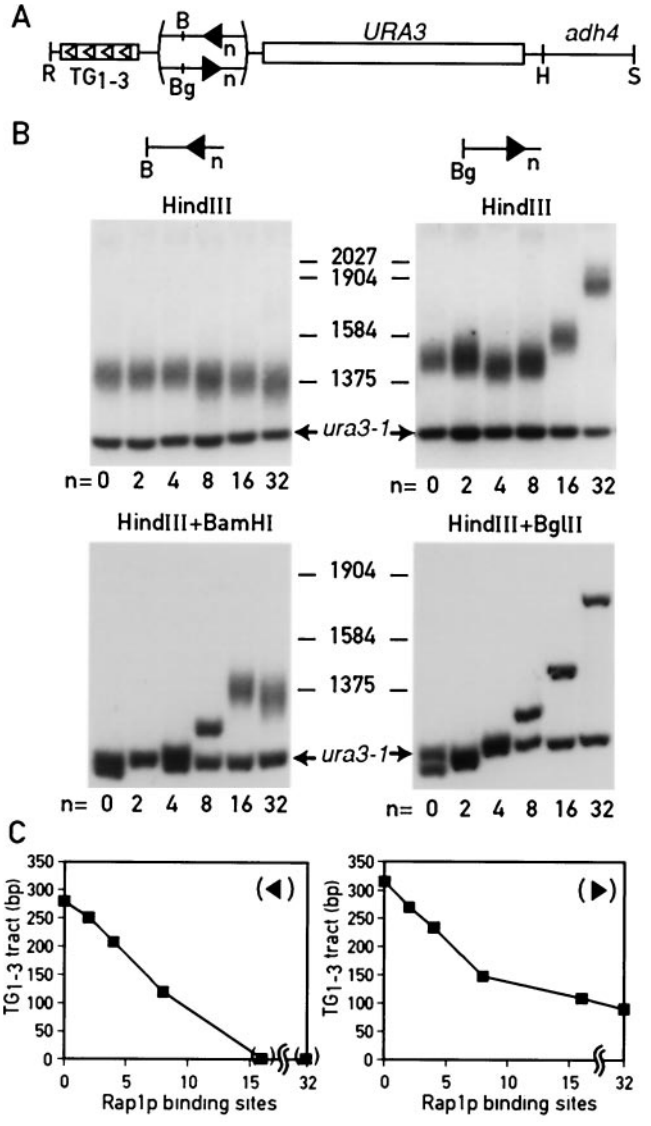

FIG. 1. Effect of the Rap1p binding site number and orientation on telomere length regulation. (A) Schematic representation of constructs used to generate a new telomere at the *ADH4* locus on chromosome VII-L (see Materials and Methods for details). The solid arrowheads represent synthetic Rap1p binding sites (n, number of Rap1p sites as shown in panel B), either in the correct (pointing left) or incorrect orientation. The unit oligonucleotide in these arrays contains two Rap1p binding sites, with an alternating 15- and 20-bp spacing between adjacent sites. The four open arrowheads represent 80 bp of TG_{1-3} sequence at the end of the healing substrate. R, *Eco*RI; B, *Bam*HI; Bg, *Bgl*II; H, *Hin*dIII; S, *Sal*I. (B) Southern blot analysis of telomeres generated from *Eco*RI-*Sal*I fragments shown in panel A containing the indicated number of Rap1p sites, either correctly oriented (left) or misoriented (right). The *URA3* probe detects the endogenous *ura3-1* locus and a diffuse telomeric band in the case of *Hin*dIII digest (top). To probe for the presence of the distal restriction site on the arrays (*Bam*HI or *Bgl*II), the appropriate double digests were examined (bottom). (C) Results of the analysis in panel B are shown graphically. The average length of the TG_{1-3} tract is plotted as a function of the number of binding sites present in the transforming constructs (see the text for explanation).

of the average amount of TG_{1-3} repeat present on the healed telomeres.

In the case of the correctly oriented arrays (Fig. 1B, left), the *Hin*dIII telomeric *URA3* fragments generated from different synthetic arrays were very similar in length (≈1,350 to 1,400 bp, corresponding to 250 to 300 bp of TG_{1-3} repeat) and essentially identical to the wild-type telomere formed by TG_{1-3} repeat sequence alone. The presence of the synthetic Rap1p binding sites in these telomeres, at least those generated from arrays with two, four, or eight binding sites, was confirmed by the presence of discrete *Hin*dIII-*Bam*HI fragments of the expected size. The fact that the sums of the lengths of the synthetic arrays plus the distal TG_{1-3} tract are very similar in every case indicates that the cell recognizes these synthetic Rap1p arrays as being essentially identical to endogenous TG_{1-3} repeats with respect to telomere length regulation. For the constructs with either 16 or 32 binding sites, the *Hin*dIII-*Bam*HI and *Hin*dIII fragments were indistinguishable, suggesting that the normal processes of telomere shortening and telomerase elongation had removed (at least) the ends of the synthetic arrays in these two cases and replaced them with TG_{1-3} repeat sequence.

Another way of expressing these results (Fig. 1C, left) is to plot the number of Rap1p binding sites in the synthetic array versus the length of TG_{1-3} repeat sequence in the resulting telomere, which is given by the *Hin*dIII fragment length minus the *Hin*dIII-*Bam*HI fragment length. This shows that there is an inverse-linear relationship between the number of synthetic sites and the amount of TG_{1-3} repeat, at least for telomeres made from arrays of two, four, or eight Rap1p sites, where this calculation can be made. Specifically, we find that for each additional synthetic Rap1p binding site added to the array there is a corresponding "loss" of approximately 18 bp of distal TG_{1-3} repeat sequence. This value is remarkably close to the estimated density of Rap1p binding sites in native TG_{1-3} repeat sequence that was derived from biochemical experiments (11). The slight telomere shortening observed for the constructs containing 8, 16, or 32 synthetic sites, relative to those with fewer or no such sites, suggests that the average site spacing in the synthetic arrays (17.5 bp per site) is slightly shorter than that which actually occurs in native repeats. To be certain that Rap1p binding, rather than some other unknown feature of these arrays, was responsible for the measured effect on TG_{1-3} repeat addition, we constructed and tested a series of mutated versions of this oligonucleotide in which the middle cytosine at each of the two C_3 stretches was changed to a guanine, which abolishes Rap1p binding. Transformation with mutant arrays containing 2, 4, 8, 16, or 32 sites, followed by the 80-bp TG_{1-3} repeat seed, yielded telomeres that retained all of the synthetic sites, followed in each case by 250 to 300 bp of TG_{1-3} repeat (data not shown). Apparently these mutant arrays, though very similar in sequence to the original arrays and having the same TG/CA strand bias, are not recognized as part of the telomeric TG_{1-3} repeat tract.

Rap1p binding site orientation is important only at the distal end of the telomere. An analysis of telomeres derived from the misoriented arrays (Fig. 1B, right) revealed both similarities and differences in comparison to the correctly oriented arrays. Arrays containing two, four, or eight misoriented sites behaved indistinguishably from the corresponding cor-

rectly oriented arrays. It thus appears that the telomere length regulatory machinery treats these arrays of misoriented sites, in one case constituting about one-half of the telomere, as if they were correctly oriented native TG_{1-3} repeats. Strikingly, however, constructs with 16 and 32 misoriented sites generated abnormally elongated telomeres that contained the complete synthetic site array, as judged by the presence of a *Bgl*II site at the same position as in the original transforming DNA (Fig. 1B, bottom right, and data not shown). In both cases, these telomeres appeared to also contain a terminal cap of TG_{1-3} repeat about 100 bp in length. This deviation from a linear relationship between the number of Rap1p binding sites in the synthetic array and TG_{1-3} tract length is shown graphically in Fig. 1C, right. These observations indicate that the telomere length regulatory machinery recognizes a long array of misoriented Rap1p binding sites as being different from an identical, correctly oriented array. One obvious explanation for this difference is that normal erosion of the elongated, misoriented arrays would expose a CA-rich strand running 5′ to 3′ towards the telomere end that would not provide a suitable substrate for telomerase and/or the end protection machinery. Such ends would then be lost, and only those containing the TG repeat buffer would then be present in the Southern blots. A more detailed analysis of these abnormal telomeres will be presented elsewhere.

Effect of altered Rap1p binding site spacing on telomere length regulation. The correctly oriented alternating 15- and 20-bp spacing arrays of Rap1p binding sites described above appear to be recognized remarkably well as normal telomeric DNA. To investigate whether this is due to some unique sequence or spacing feature of the oligonucleotide used to assemble these arrays, we generated and tested four sets of different arrays. Using the same cloning strategy, this time with oligonucleotides encoding a single Rap1p binding site, we created correctly oriented arrays with site-to-site spacing of 17, 22, 27, and 31 bp. For each oligonucleotide, constructs with one, two, four, and eight sites were generated, and in several cases 6-mer, 12-mer, and 16-mer arrays were also made. In every case, the arrays were followed by a short (80-bp) tract of genuine TG_{1-3} seed sequence, as before (Fig. 2, top). The new sites again conformed to consensus sequences and were identical to the original dimer oligonucleotide sites within the more conserved first half-site (17) but differed slightly at the end of the second half-site. Despite these slight differences, the new sites bound Rap1p in vitro with affinities indistinguishable from that of the original dimer site, with one exception (data not shown; see below).

All of these new constructs generated Ura^+ colonies at frequencies similar to that of the original dimer site arrays (data not shown). For each construct, several independent transformants were examined by Southern blotting, as described above, in order to determine the average telomere length and to probe for the presence of the *Bam*HI site at the distal end of the synthetic site array. The results of this telomere length analysis are shown graphically in Fig. 2 (bottom), where the calculated TG_{1-3} repeat length is plotted against the number of synthetic Rap1p binding sites in the array, as in Fig. 1C.

In marked contrast to the results obtained with the 15- and 20-bp spacing arrays, the 17- and 31- bp spacing arrays had little or no effect on the amount of TG_{1-3} in the healed telomeres, which in every case were in the range of ≈200 to 300 bp. It would appear, therefore, that these particular synthetic arrays of Rap1p binding sites are not recognized as part of the TG_{1-3} tract by the telomere length regulatory system, or only minimally so. The failure of the 17-bp array to support proper length regulation is likely to be a consequence of reduced Rap1p binding to these sites (data not shown), possibly due to steric hindrance at this particular site phasing (16; D. Rhodes, personal communication). The small but reproducible loss of ≈5 to 10 bp of TG_{1-3} repeat per site for these constructs might be explained by occupancy of alternating sites in this array. Interestingly, Ray and Runge (46) found that a particular 6-mer array of Rap1p sites with an even smaller site spacing (13 bp) could be counted normally. However, this observation is consistent with a prediction from the structural studies that a 13-bp spacing between sites, unlike the 17-bp spacing, should accommodate continuous Rap1p binding (D. Rhodes, personal communication). The failure to detect a strong response of the system to the 31-bp spacing array is somewhat surprising in light of the finding that a 6-mer array of Rap1p binding sites with a spacing of 35 bp can be efficiently counted (46). We do not know the reason for this apparent discrepancy, but one possibility might be that the rotational disposition of sites on the 31-bp array is unfavorable. Alternatively, some other sequence feature of this site, unrelated to its ability to bind Rap1p, might prevent its recognition as a telomeric sequence.

The 22- and 27-bp spacing arrays, though, gave a roughly proportional decrease in added TG_{1-3} repeat as the number of synthetic sites increased from one to eight. We conclude from this that site spacings of 22 and 27 bp are consistent with

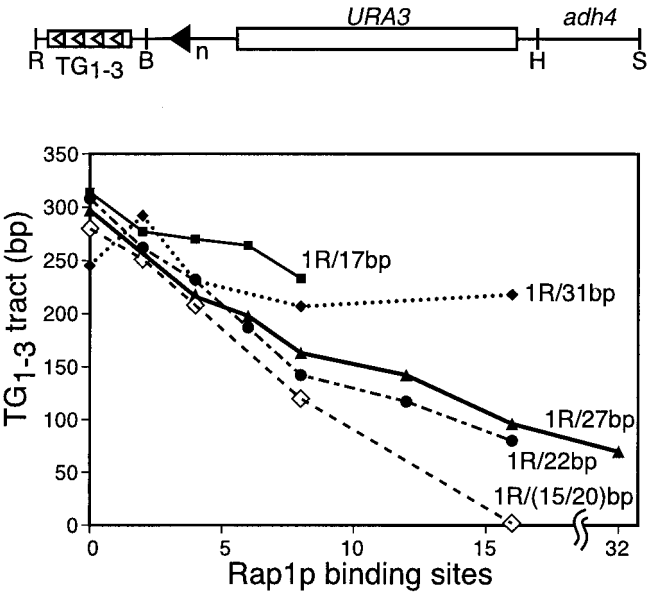

FIG. 2. The effect of Rap1p binding site spacing on telomere length regulation. (Top) Schematic representation of the constructs used to generate a novel telomere at chromosome VII-L (Fig. 1). Arrays of 2 to 32 (n) Rap1p binding sites with site-to-site spacing of 17, 22, 27, or 31 bp (see Materials and Methods) were created. See the legend to Fig. 1 for definitions of symbols. (Bottom) Telomeres generated from the constructs shown (top) were analyzed by Southern blotting, and the results of this analysis are shown graphically (as in Fig. 1C).

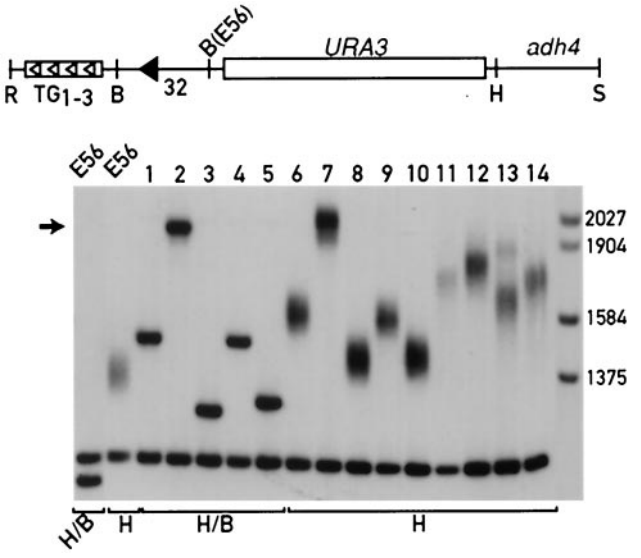

FIG. 3. Long telomeres containing 32 Rap1p binding sites at a density of 1 site per 27 bp shorten by internal deletion of synthetic sites. (Top) Schematic representation of the relevant parts of plasmid pE243, which contains 32 synthetic Rap1p binding sites with site-to-site spacing of 27 bp. See the legend to Fig. 1 for definitions of symbols. (Bottom) Lanes 1 to 10, telomeres from five independent Ura^+ transformants obtained with *Eco*RI/*Sal*I-digested pE243 were analyzed following *Hin*dIII/*Bam*HI digestion (lanes 1 to 5) or *Hin*dIII digestion (lanes 6 to 10) of the same samples. Lanes marked E56 contain genomic DNA from a strain lacking synthetic sites but containing adjacent *Bam*HI and *Bgl*II sites between *URA3* and the $TG_{1–3}$ tract. Lanes 11 to 14, telomeres from four independent Ura^+ transformants obtained by transformation with a *Sal*I/*Bam*HI fragment of pE243 were analyzed after *Hin*dIII digestion. The arrow to the left of the autoradiogram indicates the size of the pE243 *Hin*dIII-*Bam*HI fragment.

recognition by the "counting" mechanism, at least for arrays up to eight sites long, which occupy the centromere-proximal half of the telomere. However, we consistently noted a slight deviation in the inverse-linear relationship between site number and amount of $TG_{1–3}$ repeat added for the two longer arrays (12 or 16 sites) of the 22- and 27-bp spacing oligonucleotides. Whereas a 16-site array of the 15- and 20-bp spacing oligonucleotide was recognized as a complete telomere, the same number of synthetic binding sites present in the 22- or 27-bp spacing arrays always generated telomeres with ≈100 bp of additional $TG_{1–3}$ repeat (Fig. 2), all of which retained the *Bam*HI site at the end of the array (data not shown).

Abnormal telomere length regulation in long Rap1p binding site arrays points to an end-specific defect. To investigate further the apparently altered length regulation properties of the 22- and 27-bp spacing arrays, we constructed a much longer (32-mer) array with the 27-bp spacing sites (Fig. 3, top). This array contained approximately twice the number of Rap1p binding sites present at an average-length native telomere and was capped by an 80-bp native $TG_{1–3}$ sequence. If the 27-bp spacing sites could be counted, at least to some extent, one might expect to observe telomeres shorter than the 32-mer array itself in which the distal *Bam*HI site would be lost in the process of telomere shortening. Alternatively, if the 32 sites in this array are still not sufficient to constitute a stable telomere, one might imagine that telomerase-generated repeats (or the 80-bp $TG_{1–3}$ seed at the end) would make up the missing information and allow for the generation of a stable, though abnormally long, telomere array.

As shown in Fig. 3 (bottom), however, a quite different result was obtained with the 32-mer array. Telomere healing was efficient with this construct but led to the generation of individual clones with remarkably different average telomere lengths. What was particularly striking was that most of the novel telomeres examined (13 of 15 [Fig. 3 and data not shown]), regardless of length, retained the *Bam*HI site at the distal end of the synthetic site array and appeared to be capped by ≈50 to 100 bp of $TG_{1–3}$ sequence. Because many of these telomeres were shorter than the original 32-mer array itself, it appeared that shortening had occurred not by deletion from the end but rather by an internal loss of sequences within the 32-mer array. The repetitive nature of the arrays suggests that this might have occurred through a homology-dependent mechanism. In any event, the behavior of this 27-bp spacing array was clearly different from that seen with the 15- and 20-bp spacing arrays, where constructs with 16 or 32 sites rapidly generated normal-length telomeres through a mechanism that removed sequences from the end of the array (Fig. 1 and data not shown). Despite the inability of the 27-bp spacing array to shorten in a normal fashion, this array by itself (that is, lacking an 80-bp $TG_{1–3}$ cap) can act as a substrate for telomere formation in the transformation assay (Fig. 3, lanes 11 to 14). Taken together, these data point to an end-specific function that is absent or at least partially defective in the 22- and 27-bp spacing arrays but intact in the 15- or 20-bp spacing array. This function is unlikely to be related to Rap1p binding per se but instead may reflect stringent sequence requirements for an end-specific factor(s) required for proper regulation of telomerase access or activity or for telomere end protection (see Results and Discussion). Although the 22- and 27-bp arrays differ in sequence from the 15- and 20-bp spacing array in both the spacer regions and part of the Rap1p binding site itself, we do not know at present which difference(s) causes their altered behavior.

Misoriented Rap1p binding sites can contribute to telomere formation. In addition to their role in telomere length regulation, Rap1p binding sites and the Rap1p carboxy terminus are known to promote de novo telomere formation in transformation-based telomere-healing assays (30, 31, 45) by an unknown mechanism(s). Given that inverted Rap1p binding site arrays within the centromere-proximal part of a telomere can be counted by the length regulation system (Fig. 1), we asked whether they might also contribute quantitatively to telomere formation, provided that correctly oriented sites were present at the end of the array. Figure 4A shows that this is indeed the case. As little as one correctly oriented site at the end of a long (16-mer) array of misoriented sites allowed for very efficient telomere formation. In all cases examined (Fig. 4A and data not shown), misoriented sites make a quantitative contribution to healing efficiency similar to that observed for correctly oriented sites. As expected (39), arrays containing only misoriented Rap1p binding sites completely fail to form telomeres in this assay (data not shown).

Despite the high efficiency at which telomeres are generated from these mixed-orientation arrays, Southern blot analysis

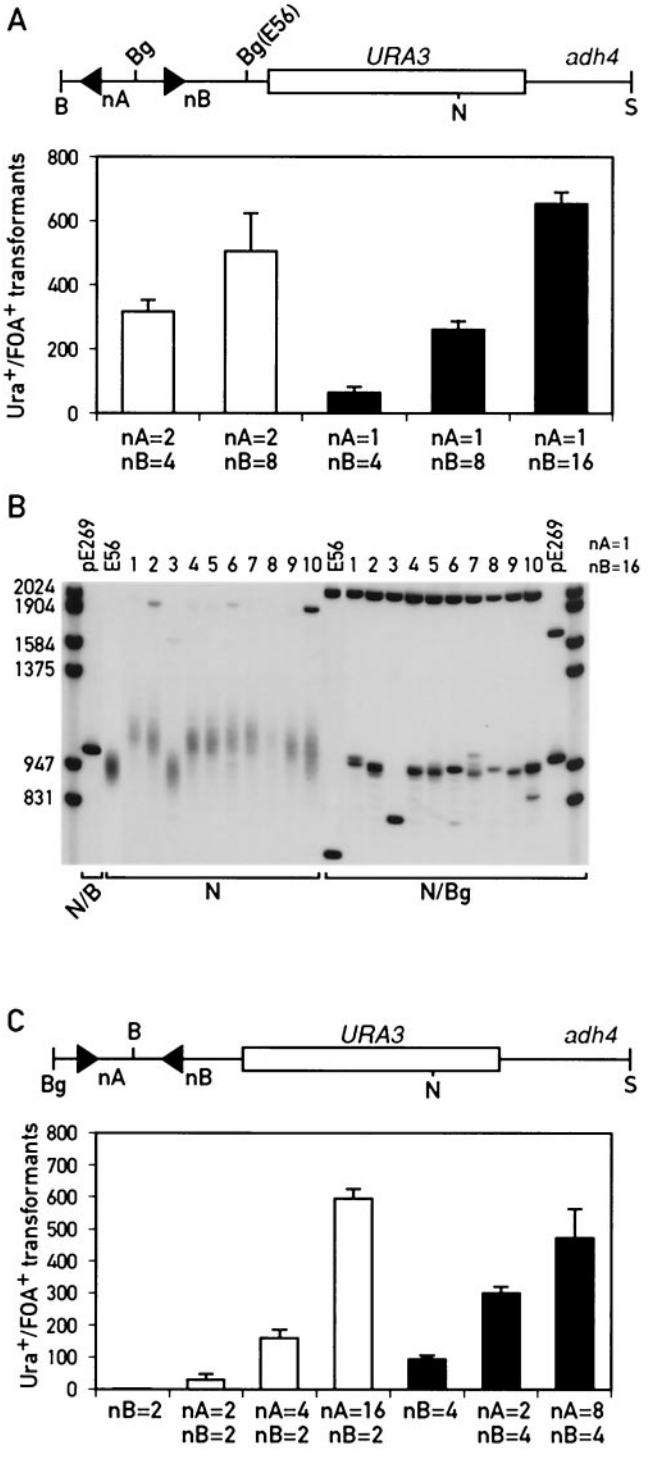

FIG. 4. Misoriented Rap1p binding sites contribute to telomere formation in combination with correctly oriented sites. (A) Schematic representations of mixed-array telomere-healing constructs (top). N, *Nco*I; B, *Bam*HI; Bg, *Bgl*II; S, *Sal*I. The solid arrows represent synthetic 15- and 20-bp spacing Rap1p binding sites (nA, number of distal Rap1p binding sites, pointing left; nB, number of proximal Rap1p binging sites, pointing right), either in the native or in the opposite orientation, except for the distal site nA = 1, which is derived from the monomer 22-bp spacing site. The number of Ura^+ and FOA^+ transformants generated with *Bam*HI/*Sal*I fragments is plotted as a function of array length and orientation (bottom). Open bars, nA = 2; solid bars, nA = 1. (B) Lanes 1 to 10, telomeres from 10 independent Ura^+ transformants generated by pE269 (nA = 1; nB = 16) were analyzed as described in the legend to Fig. 1B, except that *Nco*I digestion was used instead of *Hin*dIII. The lanes marked E56 contain DNA from cells with only adjacent *Bam*HI and *Bgl*II sites between the TG_{1-3} telomeric tract and *URA3*. (C) Telomere-healing efficiency (bottom), measured as for panel A, for a series of constructs containing terminal misoriented Rap1p binding sites (top). Open bars, nB = 2; solid bars, nB = 4.

indicates that their structure and length regulation is often abnormal. For example, telomeres generated from the construct with 16 misoriented sites and a single correctly oriented terminal site are slightly longer on average and considerably more heterogeneous than telomeres generated by a natural TG_{1-3} seed sequence alone (Fig. 4B). Remarkably, the *Bgl*II restriction site between the incorrectly and correctly oriented arrays is present in most telomeres but displaced slightly towards the proximal end of the array. In one example (Fig. 4B, clone 3), this movement was more dramatic, and the resulting telomeres in this case more closely resemble wild-type telomeres in average length and distribution. This shortening of the internal portion of the telomere array is reminiscent of the behavior of the long (32-mer) arrays of 27-bp spacing sites (Fig. 3) and is suggestive of a high rate of recombinational rearrangement not observed with the correctly oriented 15- and 20-bp spacing arrays.

Efficient telomere formation by distal misoriented Rap1p binding sites is associated with array rearrangements. Taken together, the results described above suggest that telomere formation might not occur at all with constructs containing misoriented Rap1p binding sites at the terminus. We tested this idea and found that it is not true. As shown in Fig. 4C, several different types of arrays with distal misoriented sites readily generated stable transformants. Although these reactions were not as efficient on a per-site basis as arrays with correctly oriented termini, a clear increase in efficiency was observed as the numbers of misoriented sites increased.

Surprisingly, none of the telomeres that resulted from these healing reactions retained the internal *Bam*HI restriction site separating the distal misoriented arrays from the proximal, correctly oriented arrays (see below). One explanation for this result is that the external misoriented sites had been lost in the process of telomere formation, either by exonucleolytic degradation or incomplete replication. However, it is difficult to imagine how misoriented sites could contribute to telomere formation if they are lost in the process. We therefore considered an alternative hypothesis, namely that a recombinational rearrangement of the mixed arrays occurs at some point during telomere formation such that the restriction site between the two arrays ends up at a more distal position. This site might then be lost, either through normal sequence turnover at the distal end of the telomere or through a more directed nucleolytic process (see Discussion). A schematic representation of how this might occur is shown in Fig. 5, where we consider the possibility of either intermolecular reactions between sister chromatids (Fig. 5A) or intramolecular events (Fig. 5B).

A key prediction of these recombinational models is that an external restriction site placed within the misoriented array (*Bgl*II) would assume a more internal position after the rearrangement relative to the (originally) internal site (*Bam*HI)

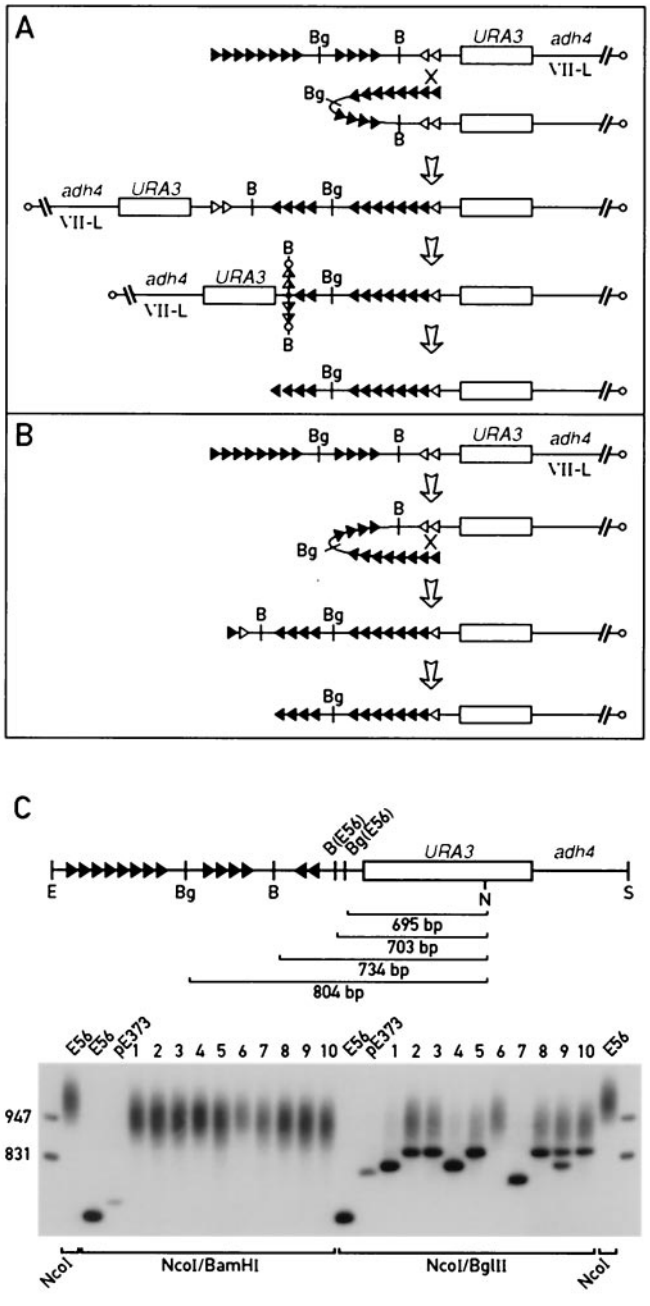

FIG. 5. Telomere formation by mixed-orientation Rap1p site arrays occurs through array rearrangement. Models involving intermolecular (A) or intramolecular (B) recombination pathways that could explain the role of misoriented terminal Rap1p binding sites in telomere formation. Open and solid arrowheads in the original transforming DNA represent correctly oriented and misoriented Rap1p binding sites, respectively. (C) Experimental evidence that telomere formation by arrays terminating in misoriented Rap1p binding sites occurs through a process of array inversion. (Top) Schematic representation of the healing construct pE373, in which the external array of misoriented Rap1p binding sites contains an intervening *Bgl*II restriction site (B, *Bam*HI; Bg, *Bgl*II; N, *Nco*I; S, *Sal*I). The *Bam*HI and *Bgl*II sites in the control parental vector (pE56) are shown for reference. (Bottom) Lanes 1 to 10, telomeres from 10 independent Ura$^+$ transformants of pE373 were analyzed by Southern blotting, after digestion with the indicated enzymes, using a *URA3* probe. Genomic DNA from a transformant with pE56 and digests of pE373 plasmid DNA are shown for size references.

separating the two arrays. We therefore constructed and tested a healing substrate of this type. Southern blot analysis of the telomeres resulting from this construct (Fig. 5C) gave a result in striking accord with the recombination models outlined above. In all (10 of 10) of the telomeres analyzed, the (centromere-proximal) *Bam*HI site was lost, despite the fact that in most cases (9 of 10) the more distal *Bgl*II site, within the misoriented array, was still present, at least in a fraction of the telomeres from each culture. In those cases where the *Bgl*II site has been lost, it seems likely that this has occurred through the normal process of sequence turnover at the telomere end. Consistent with this interpretation, those transformants in which the *Bgl*II site is located in a more proximal position (Fig. 5C, lanes 1, 4, and 7) display the smallest fraction of telomeres in which the site is no longer present. In summary, these data are thus inconsistent with models in which the misoriented sites are lost during the healing process itself.

Evidence that telomere formation by site rearrangement occurs at a step following chromosomal integration. The presumptive recombination reactions that led to the telomeres shown in Fig. 5C might have occurred during the transformation process itself, with the exogenously added DNA serving as the substrate. Alternatively, rearrangement might proceed following integration of the transforming DNA into the chromosome, by either sister chromatid interactions (Fig. 5A) or an intrachromatid "loop inversion" reaction (Fig. 5B). To try to distinguish between these two possibilities, we performed a cotransformation experiment using the two DNA molecules diagrammed in Fig. 6B. In this reaction, only one fragment contains homology to sequences in the host strain (*ADH4*) and is thus capable of chromosomal integration. However, this fragment contains only two terminal Rap1p binding sites and is thus unable to promote efficient telomere formation by itself. The cotransforming DNA, however, contains two correctly oriented Rap1p sites followed by a long (8-mer) array of misoriented sites that could, in principle, recombine with the short array on the first fragment to generate a stable telomere through a mechanism(s) such as those outlined in Fig. 5. Because the *URA3* gene was deleted in the host strain, this fragment could not form Ura$^+$ colonies through any mechanism involving homologous recombination. As shown in Fig. 6B, this cotransformation yielded many fewer colonies (≈100-fold less) than the original mixed-array control transformation (Fig. 6A), suggesting that intermolecular recombination of the transforming DNA itself is not a major pathway for telomere formation in this system. Nonetheless, the transformants that were obtained are likely to have resulted from intermolecular recombination events, since control transformations with either single molecule failed to yield any transformants (data not shown). Interestingly, when an array "donor" containing only misoriented sites fused to the *URA3* gene was used in the cotransformation, no transformants were obtained (Fig. 6C). This observation suggests that the apposition of correctly oriented and misoriented sites in a donor molecule (Fig. 6B) may promote the resolution of recombinant molecules into stable telomeres (see Discussion).

A *RAD52*-dependent fusion breakage pathway for telomere formation from mixed Rap1p binding site arrays. To examine the process of telomere formation from these mixed Rap1p binding site arrays in more detail, we turned to a different assay

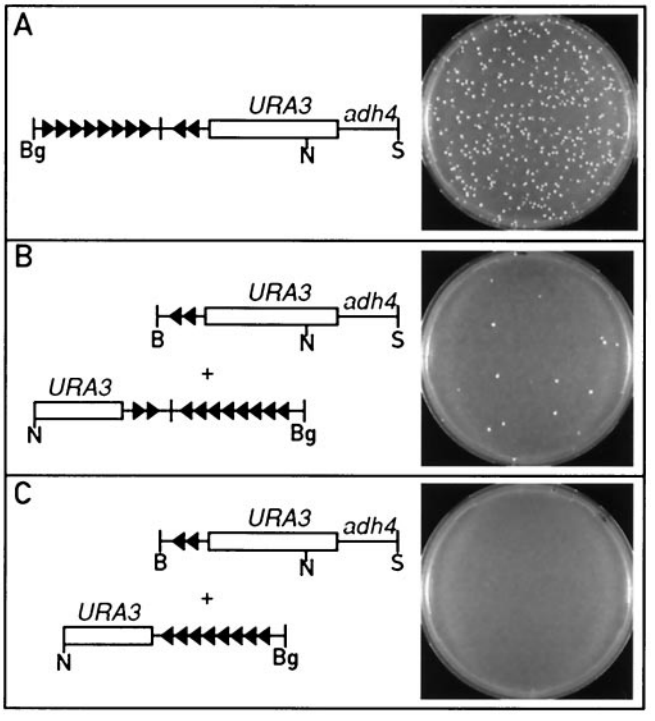

FIG. 6. Telomere formation is not promoted by bimolecular interactions between transforming DNA molecules containing Rap1p site arrays. (A) Mixed-orientation construct (similar to that shown in Fig. 5C) and a representative transformation plate (SC-Ura) derived from this DNA. (B) Two DNA molecules used in a cotransformation assay, the results of which are shown on the right. (C) Cotransformation similar to that depicted in panel B but in which the donor DNA molecule (containing a truncated *URA3* gene) lacks an internal head-to-head arrangement of Rap1p binding sites. See the legend to Fig. 5 for definitions of symbols.

in which telomeres are generated at a unique chromosomal break created by HO endonuclease cleavage (see Materials and Methods). A similar telomere formation assay has been described recently by Diede and Gottschling (8). One advantage of the HO cleavage assay over the transformation system is that a much larger fraction of cells in the culture undergo telomere formation, owing to the fact that HO cutting is considerably more efficient than DNA transformation and subsequent homologous recombination. Consequently, telomere formation in the HO assay can be examined directly by Southern blotting.

The results of such an assay using a substrate analogous to the mixed-array molecule described previously are shown in Fig. 7. Several features of this healing reaction are worth emphasizing. First, although HO cleavage was essentially complete by 4 to 6 h (Fig. 7C and data not shown), the final heterogeneous distribution of telomere products was not present in significant amounts until sometime after 21 h. Second, and of particular importance here, is the appearance in the *Bst*XI-digested samples of a complex set of bands following HO cleavage (Fig. 7C). These bands, ranging in size between ≈1.1 and 1.3 kb, correspond to the sizes predicted for the joining of two chromatids by homologous exchange between a misoriented and a correctly oriented array after HO cutting (Fig. 5A and 7B). Significantly, these putative recombinant molecules disappeared as the final telomere products appeared, strongly suggesting that they were intermediates in the telomere formation process. Supporting this proposition, we observed the simultaneous appearance of a novel set of *Bst*XI-*Bgl*II bands consistent with homologous recombination between different arrays at a select number of registers within the arrays. As predicted by the proposed resolution mechanism, following homologous exchange between arrays, these *Bst*XI-*Bgl*II bands persist in the final healed telomeres. Also consistent with the recombination models in Fig. 5 is the transient appearance of a set of *Bam*HI sites at positions corresponding to the eventual telomere ends (Fig. 7C, *Bst*XI/*Bam*HI digest). These *Bam*HI sites are predicted to be the sites of a resolution reaction that generates an end suitable for telomerase access and proper end protection (Fig. 5A).

An additional advantage of the HO cut assay is that it does not impose any obvious requirement for recombination. Consistent with this notion, telomere formation from HO breaks adjacent to correctly oriented arrays of Rap1p binding sites is completely independent of *RAD52* function (data not shown). Strikingly, however, telomere formation from the mixed-orientation Rap1p arrays is largely blocked by deletion of *RAD52*, and none of the purported intermediates in this process are detected following HO cleavage (Fig. 7D). These genetic data indicate a unique requirement for recombination in telomere formation from the mixed arrays and support our claim that the molecules observed by Southern blot analysis during telomere formation from these substrates are in fact recombination intermediates.

DISCUSSION

We have used synthetic arrays of Rap1p binding sites in telomere-healing assays to explore the role of Rap1p in de novo telomere formation and telomere length regulation. Although our results are broadly consistent with a model in which the number of Rap1p molecules bound to the chromosome end serves as a measure of telomere length (34, 46, 48), they also point to special sequence constraints at the very end of the telomere repeat array, apparently unrelated to Rap1p binding, that are critical for normal telomere homeostasis. In the absence of a proper telomere end DNA structure, two different responses were observed. In one case, a buffer of genuine TG_{1-3} was consistently found on telomeres with abnormally long (but unstable) arrays of Rap1p binding sites. Remarkably, in cases where mixed-orientation arrays terminated with misoriented Rap1p binding sites, an active recombinational process, apparently involving end-to-end fusion and subsequent resolution of sister chromatids, was able to efficiently restore a proper telomere end structure.

Effect of Rap1p site spacing and orientation on telomere length sensing. By varying the total number and spacing between synthetic Rap1p binding sites in different telomere-healing constructs, we have been able to test more rigorously the idea that telomeric TG_{1-3} repeat tract length is sensed and regulated according to the number of bound Rap1p molecules (34, 45, 46). Telomere length measurements show that for Rap1p binding site arrays containing up to at least eight sites, and with site-to-site spacing of 15 and 20, 22, or 27 bp, there is

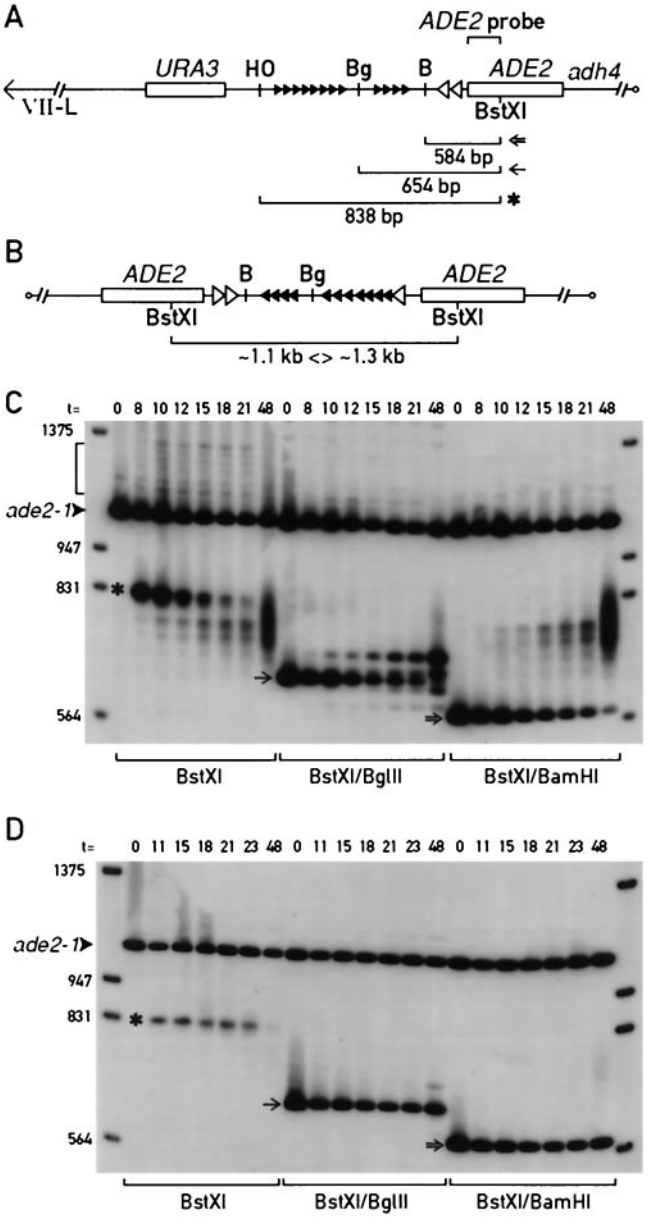

FIG. 7. Telomere formation from mixed-orientation Rap1p site arrays at a chromosome break: evidence for *RAD52*-dependent recombination intermediates. (A) Schematic representation of the chromosome VII-L telomere in which the region spanning the *MNT2* and *ADH4* loci has been replaced by a DNA fragment containing the *URA3* gene, an HO cut site, an array of mixed-orientation Rap1p binding sites (Fig. 5), and the *ADE2* gene. The expected sizes of *Bst*XI-*Bam*HI, *Bst*XI-*Bgl*II, and *Bst*XI-HO fragments detected by the 0.5-kb *ADE2* probe are indicated. (B) Schematic representation of predicted intermediate(s) resulting from head-to-head joining of HO-cut sister chromatids by homologous recombination within Rap1p site arrays (Fig. 5A). The size range of novel *Bst*XI fragments is indicated below the diagram. (C) Southern blot analysis of the kinetics of telomere formation in strain YS293 following galactose induction of HO for the indicated time (t, in hours). The blot was probed with the 0.5-kb *ADE2* fragment indicated in panel A. The asterisk indicates the *Bst*XI fragment generated following HO cleavage (the ≈13-kb *Bst*XI fragment present before HO cutting is not shown on this blot), the solid arrow shows the position of the original *Bst*XI-*Bgl*II fragment, and the open arrow indicates the original *Bst*XI-*Bam*HI fragment. The bracket on the left indicates the position of a set of *Bst*XI fragments that arise following HO cutting (see panel B). (D) Southern blot analysis of chromosome VII-L telomeres from the *rad52*::*KanMX* mutant strain YS312 (otherwise isogenic to YS293) following galactose induction of HO, as for panel C.

a quantitative inverse-linear relationship between the number of sites in an array and the amount of TG_{1-3} repeat sequence added by telomerase after transformation and integration. In other words, the telomere length regulatory mechanism responds to the number of Rap1p binding sites within the arrays and not to their length per se, at least over this range of site spacing. Our measured value of the TG_{1-3} repeat length equivalent for a single synthetic Rap1p binding site is approximately 16 to 20 bp, very similar to the average spacing between Rap1p molecules estimated from in vitro measurements on genuine telomeric TG_{1-3} repeat DNA (11). Finally, we note that the orientation of sites in this range (one to eight sites) had no significant impact on their ability to be counted. These conclusions are consistent with previous work in which either 80 or 270 bp of genuine telomere tract DNA or arrays of six Rap1p binding sites (both either correctly oriented or misoriented) were examined (34, 45, 46). In the present study, we found that Rap1p sites within arrays with site spacings of 17 or 31 bp did not effectively contribute to telomere length regulation. In the former case, poor binding in vitro by Rap1p (data not shown), probably due to steric hindrance between adjacent sites, could easily explain the in vivo result. However, the 31-bp spacing arrays bind Rap1p in vitro with high affinity, so their failure to participate efficiently in telomere length regulation must be due to some other sequence feature of these arrays, or perhaps to the rotational disposition of the Rap1p binding sites. It seems unlikely that the longer distance between sites is responsible for the loss of function, since a 6-mer array of Rap1p sites with an even larger spacing (35 bp) contributed normally to telomere length regulation (46).

Unique properties of the distal ends of telomere arrays: evidence for a capping function with stringent DNA sequence requirements. By extending the synthetic Rap1p binding site arrays to include 16 or 32 sites, we discovered a striking difference between the behavior of the 15- and 20-bp spacing array and the two other well-counted arrays (22- and 27-bp spacing). In the former case, we consistently observed efficient formation of normal-length telomeres, where the distal restriction site at the end of the synthetic array was lost. This suggests, particularly for the case of the 32-mer, that the synthetic array had blocked telomerase addition and shortened through a normal process of sequence turnover involving loss of sites from the end. This type of gradual end erosion has been observed under several different circumstances, for example, in the absence of telomerase (29) or when telomere arrays elongated by temporary exposure to a *rap1-17* mutant background are allowed to return to normal length in a wild-type cell (22, 33). In contrast, the 16-mer and 32-mer arrays with 22- or 27-bp spacing typically formed abnormally long telomeres (Fig. 3 and data not shown). Furthermore, even though telomeres formed from the 32-mer array were often shorter than the original array, they did not appear to have shortened by sequence loss from the end, since in almost all cases they had retained the distal restriction site on the original array. Instead,

these elongated telomeres are more likely to have shortened through a recombinational mechanism such as telomere rapid deletion (24).

How can one explain this dramatic difference between the 15- and 20-bp spacing array and the 22- or 27-bp spacing arrays? Perhaps the simplest explanation would be that the length-sensing mechanism breaks down for the 22- and 27-bp spacing arrays as their site numbers approach that of a native telomere. This might result from physical constraints on a folded protein-DNA complex generated by the arrays, Rap1p, and additional interacting factors (e.g., the Rif proteins). Even if this were the case, we note that the cells would appear to distinguish the 32-mer arrays from the 16-mers, since they consistently add a smaller amount of TG_{1-3} repeat to the former than to the latter (data not shown). This observation suggests that the longer arrays are sensed as having more Rap1p binding sites than the shorter ones but that they may never be sensed as having either their actual number of sites or even the minimal number (≈15 or 16 sites) normally required for length homeostasis. A second model would hold that the 22- and 27-bp arrays do not support efficient telomerase addition. According to this idea, when these sequences are exposed at a telomere end, that end will not be able to act as a telomerase substrate. Consequently, such telomeres will then undergo a process of gradual attrition like that which occurs in mutants lacking telomerase. This explanation seems unlikely for several reasons. First, we do not observe a subpopulation of telomeres undergoing gradual shortening (as is seen in *EST* mutants), so one would have to propose that such telomeres are unusually unstable. In addition, we find that the 22- and 27-bp arrays are perfectly competent in telomere formation in the absence of a TG_{1-3} seed, suggesting that they can act as telomerase substrates (Fig. 3, lanes 11 to 14).

A third possible explanation for our observations, which we favor, is that an end-specific function, not directly related to Rap1p binding, is required to properly regulate telomerase or an essential end protection function. For example, both Cdc13p and Tel2p bind specifically to single-stranded TG-rich telomeric repeat DNA and are required for normal telomere length regulation (18, 19, 25, 41, 47). Either or both of these proteins might require a specific sequence at the end of the telomere array, not provided by the 22- and 27-bp spacing arrays, in order to bind or function properly. Alternatively, the 22- and 27-bp arrays might fail to form a specialized DNA structure involving the array terminus that would be required for telomerase repression, such as the t-loop, now observed in several different organisms (14, 38, 40). Whatever the precise mechanism, we propose that exposure of the 22- or 27-bp spacing sequences near the telomere end, perhaps within only the proximal part of the resected 3′ overhang (56, 57), often results in a complete loss of telomerase repression such that additional TG_{1-3} sequences are always rapidly added. A mechanism of this sort would explain the presence of the distal restriction site and a buffer of TG_{1-3} sequence that is almost always observed beyond the synthetic arrays (Fig. 3). This proposed end-specific defect of the 22- and 27-bp spacing arrays might be related to a phenomenon referred to as telomere uncapping that occurs both in *Kluyveromyces lactis* and in *S. cerevisiae* strains when certain mutated repeat sequences are added to telomere ends (20, 21, 35, 36, 44, 49). Interestingly, when wild-type repeats are then added to these mutated ends, telomere elongation is arrested. However, these capped telomeres do not return to their normal length but instead retain the added wild-type terminal cap (21, 49), analogous to the TG_{1-3} sequence that caps the 22- and 27-bp arrays in our experiments. The parallel between these two systems lends appeal to the capping idea, but it should be pointed out that the precise molecular nature of the proposed cap is still a matter of speculation (3). We would also note that this proposed special property of the distal end is perfectly consistent with a model in which the cell "senses" telomere length by a mechanism that measures the number of Rap1p molecules bound along the complete TG_{1-3} tract. In the model described here, the end-specific factor(s) is required to execute telomerase regulation in response to a signal generated by array-bound Rap1p molecules.

A novel recombinational pathway promoting stable telomere formation. We were surprised to observe that distal misoriented Rap1p binding sites can contribute to the efficiency of telomere formation, since they are never found at the ends of the resulting telomeres. One possible scenario to explain this observation would be that such sites could stabilize the end, through binding of Rap1p or other factors, until their gradual loss would expose a resected G-rich 3′ overhang for Cdc13p binding and telomerase loading (10, 25, 41). However, the telomeres that result from these mixed arrays are clearly generated by a site rearrangement process that requires *RAD52* function (Fig. 7). Direct analysis of this reaction by Southern blotting strongly suggests that it proceeds through a transient intermediate involving head-to-head fusion of telomeres on sister chromatids, presumably through homologous recombination between their repeat arrays. At present, we cannot distinguish between two different models for this interchromatid reaction, one involving homologous exchange and the other based upon a break-induced replication (or break copy duplication) mechanism (32, 37). It is also important to note that we cannot exclude the possibility that some fraction of the rearrangement events we observe occur through an intramolecular pathway (Fig. 5B).

A role for recombination in either telomere formation or maintenance in yeast has been documented in several different contexts, both in the presence (9, 43, 55) and in the absence (6, 23, 28, 35, 51, 52) of functional telomerase enzyme. The telomere array rearrangement that we have described here would seem to differ from previously described telomere recombination reactions in that it apparently involves a transient, head-to-head telomere fusion intermediate. Although we still do not know how these fusions are resolved to make a functional telomere, it is interesting that in a cotransformation assay with two incomplete substrates the generation of telomeres (as measured by Ura^+ transformants) depended upon the presence of a head-to-head arrangement of Rap1p sites on the end donor molecule (compare Fig. 6B to 6C). Early studies of telomere formation demonstrated a robust mechanism for the conversion of circular plasmids to linear plasmids by resolution of head-to-head telomere arrays, possibly through cutting of a Holiday junction-like intermediate (39) (Fig. 5A). A similar mechanism may thus play a role in the later stages of telomere formation by the mixed-orientation arrays, where the fused

chromatids need to be resolved (broken apart) to expose an end containing correctly oriented Rap1p binding sites.

As mentioned above, the formation of stable, rearranged telomeres from the mixed-array substrates is an efficient reaction in both the transformation and HO cut assays, in the sense that individual cells have a high probability of giving rise to a colony in which the majority of cells have a normal telomere structure. It is interesting to compare these events to those that allow for survival of cells lacking telomerase, a process also dependent upon recombination. In the case of telomerase-deficient cells, senescence is the most common outcome, with survivors arising at a very low (and difficult to measure) frequency (6, 23, 28, 35, 51, 52). Although the reason for this difference is not clear, it might at least in part be explained by the fact that telomerase-negative cells need to successfully repair all of their 32 telomeres in order to live, whereas our experiments require that only a single telomere be healed. Another possibility, though, is that native telomere ends, even when shortening in the absence of telomerase, are more protected (capped) from recombination reactions than are terminal, misoriented Rap1p sites in telomerase-positive cells. We clearly need to know more about the proteins assembled at these two different types of telomeres before this issue can be resolved.

ACKNOWLEDGMENTS

We thank Ted Young and Odile Bronchain for their thoughtful comments on the manuscript, Rodney Rothstein and James Haber for stimulating discussions and useful suggestions, all the members of the Shore laboratory for their continued help and advice, and Nicolas Roggli for help with figures and artwork.

This work was supported by grants from the Swiss National Science Foundation and the Swiss Cancer League and by funds provided by the Canton of Geneva. A. Bianchi was supported by postdoctoral fellowships from EMBO and the Human Frontier Science Program.

REFERENCES

1. **Adams, A., D. E. Gottschling, C. A. Kaiser, and T. Stearns.** 1997. Methods in yeast genetics. Cold Spring Harbor Laboratory Press, Plainview, N.Y.
2. **Bilaud, T., C. E. Koering, E. Binet-Brasselet, K. Ancelin, A. Pollice, S. M. Gasser, and E. Gilson.** 1996. The telobox, a Myb-related telomeric DNA binding motif found in proteins from yeast, plants and human. Nucleic Acids Res. **24:**1294–1303.
3. **Blackburn, E. H.** 2000. Telomere states and cell fates. Nature **408:**53–56.
4. **Broccoli, D., A. Smogorzewska, L. Chong, and T. de Lange.** 1997. Human telomeres contain two distinct Myb-related proteins, TRF1 and TRF2. Nat. Genet. **17:**231–235.
5. **Buchman, A. R., W. J. Kimmerly, J. Rine, and R. D. Kornberg.** 1988. Two DNA-binding factors recognize specific sequences at silencers, upstream activating sequences, autonomously replicating sequences, and telomeres in *Saccharomyces cerevisiae*. Mol. Cell. Biol. **8:**210–225.
6. **Chen, Q., A. Ijpma, and C. W. Greider.** 2001. Two survivor pathways that allow growth in the absence of telomerase are generated by distinct telomere recombination events. Mol. Cell. Biol. **21:**1819–1827.
7. **Chong, L., B. van Steensel, D. Broccoli, H. Erdjument-Bromage, J. Hanish, P. Tempst, and T. de Lange.** 1995. A human telomeric protein. Science **270:**1663–1667.
8. **Diede, S. J., and D. E. Gottschling.** 1999. Telomerase-mediated telomere addition in vivo requires DNA primase and DNA polymerases alpha and delta. Cell **99:**723–733.
9. **Dunn, B., P. Szauter, M. L. Pardue, and J. W. Szostak.** 1984. Transfer of yeast telomeres to linear plasmids by recombination. Cell **39:**191–201.
10. **Evans, S. K., and V. Lundblad.** 1999. Est1 and Cdc13 as comediators of telomerase access. Science **286:**117–120.
11. **Gilson, E., M. Roberge, R. Giraldo, D. Rhodes, and S. M. Gasser.** 1993. Distortion of the DNA double helix by RAP1 at silencers and multiple telomeric binding sites. J. Mol. Biol. **231:**293–310.
12. **Gottschling, D. E., O. M. Aparicio, B. L. Billington, and V. A. Zakian.** 1990. Position effect at S. cerevisiae telomeres: reversible repression of Pol II transcription. Cell **63:**751–762.
13. **Graham, I. R., and A. Chambers.** 1994. Use of a selection technique to identify the diversity of binding sites for the yeast rap1 transcription factor. Nucleic Acids Res. **22:**124–130.
14. **Griffith, J. D., L. Comeau, S. Rosenfield, R. M. Stansel, A. Bianchi, H. Moss, and T. de Lange.** 1999. Mammalian telomeres end in a large duplex loop. Cell **97:**503–514.
15. **Hardy, C. F. J., L. Sussel, and D. Shore.** 1992. A RAP1-interacting protein involved in silencing and telomere length regulation. Genes Dev. **6:**801–814.
16. **Konig, P., L. Fairall, and D. Rhodes.** 1998. Sequence-specific DNA recognition by the myb-like domain of the human telomere binding protein TRF1: a model for the protein-DNA complex. Nucleic Acids Res. **26:**1731–1740.
17. **Konig, P., R. Giraldo, L. Chapman, and D. Rhodes.** 1996. The crystal structure of the DNA-binding domain of yeast RAP1 in complex with telomeric DNA. Cell **85:**125–136.
18. **Kota, R. S., and K. W. Runge.** 1999. Tel2p, a regulator of yeast telomeric length in vivo, binds to single-stranded telomeric DNA in vitro. Chromosoma **108:**278–290.
19. **Kota, R. S., and K. W. Runge.** 1998. The yeast telomere length regulator TEL2 encodes a protein that binds to telomeric DNA. Nucleic Acids Res. **26:**1528–1535.
20. **Krauskopf, A., and E. H. Blackburn.** 1996. Control of telomere growth by interactions of RAP1 with the most distal telomeric repeats. Nature **383:** 354–357.
21. **Krauskopf, A., and E. H. Blackburn.** 1998. Rap1 protein regulates telomere turnover in yeast. Proc. Natl. Acad. Sci. USA **95:**12486–12491.
22. **Kyrion, G., K. A. Boakye, and A. J. Lustig.** 1992. C-terminal truncation of RAP1 results in the deregulation of telomere size, stability, and function in *Saccharomyces cerevisiae*. Mol. Cell. Biol. **12:**5159–5173.
23. **Le, S., J. K. Moore, J. E. Haber, and C. W. Greider.** 1999. RAD50 and RAD51 define two pathways that collaborate to maintain telomeres in the absence of telomerase. Genetics **152:**143–152.
24. **Li, B., and A. J. Lustig.** 1996. A novel mechanism for telomere size control in *Saccharomyces cerevisiae*. Genes Dev. **10:**1310–1326.
25. **Lin, J. J., and V. A. Zakian.** 1996. The *Saccharomyces* CDC13 protein is a single-strand TG1–3 telomeric DNA-binding protein in vitro that affects telomere behavior in vivo. Proc. Natl. Acad. Sci. USA **93:**13760–13765.
26. **Longtine, M. S., N. M. Wilson, M. E. Petracek, and J. Berman.** 1989. A yeast telomere binding activity binds to two related telomere sequence motifs and is indistinguishable from RAP1. Curr. Genet. **16:**225–239.
27. **Lundblad, V.** 2000. DNA ends: maintenance of chromosome termini versus repair of double strand breaks. Mutat. Res. **451:**227–240.
28. **Lundblad, V., and E. H. Blackburn.** 1993. An alternative pathway for yeast telomere maintenance rescues *est1-* senescence. Cell **73:**347–360.
29. **Lundblad, V., and J. W. Szostak.** 1989. A mutant with a defect in telomere elongation leads to senescence in yeast. Cell **57:**633–643.
30. **Lustig, A. J.** 1992. Hoogsteen G-G base pairing is dispensable for telomere healing in yeast. Nucleic Acids Res. **20:**3021–3028.
31. **Lustig, A. J., S. Kurtz, and D. Shore.** 1990. Involvement of the silencer and UAS binding protein RAP1 in regulation of telomere length. Science **250:** 549–553.
32. **Malkova, A., E. L. Ivanov, and J. E. Haber.** 1996. Double-strand break repair in the absence of RAD51 in yeast: a possible role for break-induced DNA replication. Proc. Natl. Acad. Sci. USA **93:**7131–7136.
33. **Marcand, S., V. Brevet, and E. Gilson.** 1999. Progressive *cis*-inhibition of telomerase upon telomere elongation. EMBO J. **18:**3509–3519.
34. **Marcand, S., E. Gilson, and D. Shore.** 1997. A protein-counting mechanism for telomere length regulation in yeast. Science **275:**986–990.
35. **McEachern, M. J., and E. H. Blackburn.** 1996. Cap-prevented recombination between terminal telomeric repeat arrays (telomere CPR) maintains telomeres in *Kluyveromyces lactis* lacking telomerase. Genes Dev. **10:**1822–1834.
36. **McEachern, M. J., and E. H. Blackburn.** 1995. Runaway telomere elongation caused by telomerase RNA gene mutations. Nature **376:**403–409.
37. **Morrow, D. M., C. Connelly, and P. Hieter.** 1997. "Break copy" duplication: a model for chromosome fragment formation in *Saccharomyces cerevisiae*. Genetics **147:**371–382.
38. **Munoz-Jordan, J. L., G. A. Cross, T. Lange, and J. D. Griffith.** 2001. t-loops at trypanosome telomeres. EMBO J. **20:**579–588.
39. **Murray, A. W., T. E. Claus, and J. W. Szostak.** 1988. Characterization of two telomeric DNA processing reactions in *Saccharomyces cerevisiae.* Mol. Cell. Biol. **8:**4642–4650.
40. **Murti, K. G., and D. M. Prescott.** 1999. Telomeres of polytene chromosomes in a ciliated protozoan terminate in duplex DNA loops. Proc. Natl. Acad. Sci. USA **96:**14436–14439.
41. **Nugent, C. I., T. R. Hughes, N. F. Lue, and V. Lundblad.** 1996. Cdc13p: a single-strand telomeric DNA-binding protein with a dual role in yeast telomere maintenance. Science **274:**249–252.
42. **Nugent, C. I., and V. Lundblad.** 1998. The telomerase reverse transcriptase: components and regulation. Genes Dev. **12:**1073–1085.
43. **Pluta, A. F., and V. A. Zakian.** 1989. Recombination occurs during telomere formation in yeast. Nature **337:**429–433.
44. **Prescott, J. C., and E. H. Blackburn.** 2000. Telomerase RNA template

mutations reveal sequence-specific requirements for the activation and repression of telomerase action at telomeres. Mol. Cell. Biol. **20:**2941–2948.
45. **Ray, A., and K. W. Runge.** 1998. The C terminus of the major yeast telomere binding protein Rap1p enhances telomere formation. Mol. Cell. Biol. **18:** 1284–1295.
46. **Ray, A., and K. W. Runge.** 1999. The yeast telomere length counting machinery is sensitive to sequences at the telomere-nontelomere junction. Mol. Cell. Biol. **19:**31–45.
47. **Runge, K. W., and V. A. Zakian.** 1996. TEL2, an essential gene required for telomere length regulation and telomere position effect in *Saccharomyces cerevisiae*. Mol. Cell. Biol. **16:**3094–3105.
48. **Shore, D.** 1997. Telomere length regulation: getting the measure of chromosome ends. Biol. Chem. **378:**591–597.
49. **Smith, C. D., and E. H. Blackburn.** 1999. Uncapping and deregulation of telomeres lead to detrimental cellular consequences in yeast. J. Cell Biol. **145:**203–214.
50. **Smogorzewska, A., B. van Steensel, A. Bianchi, S. Oelmann, M. R. Schaefer, G. Schnapp, and T. de Lange.** 2000. Control of human telomere length by TRF1 and TRF2. Mol. Cell. Biol. **20:**1659–1668.
51. **Teng, S., J. Chang, B. McCowan, and V. A. Zakian.** 2000. Telomerase-independent lengthening of yeast telomeres occurs by an abrupt Rad50p-dependent, Rif-inhibited recombinational process. Mol. Cell **6:**947–952.
52. **Teng, S. C., and V. A. Zakian.** 1999. Telomere-telomere recombination is an efficient bypass pathway for telomere maintenance in *Saccharomyces cerevisiae*. Mol. Cell. Biol. **19:**8083–8093.
53. **Thomas, B. J., and R. Rothstein.** 1989. The genetic control of direct-repeat recombination in *Saccharomyces*: the effect of *rad52* and *rad1* on mitotic recombination at *GAL10*, a transcriptionally regulated gene. Genetics **123:** 725–738.
54. **van Steensel, B., and T. de Lange.** 1997. Control of telomere length by the human telomeric protein TRF1. Nature **385:**740–743.
55. **Wang, S. S., and V. A. Zakian.** 1990. Telomere-telomere recombination provides an express pathway for telomere acquisition. Nature **345:**456–458.
56. **Wellinger, R. J., K. Ethier, P. Labrecque, and V. A. Zakian.** 1996. Evidence for a new step in telomere maintenance. Cell **85:**423–433.
57. **Wellinger, R. J., A. J. Wolf, and V. A. Zakian.** 1993. Saccharomyces telomeres acquire single-strand TG1–3 tails late in S phase. Cell **72:**51–60.
58. **Wotton, D., and D. Shore.** 1997. A novel Rap1p-interacting factor, Rif2p, cooperates with Rif1p to regulate telomere length in *Saccharomyces cerevisiae.* Genes Dev. **11:**748–760.